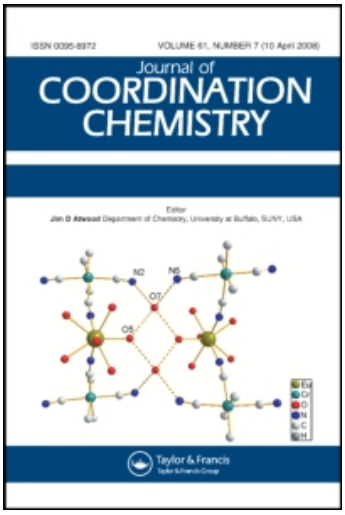

Journal of Coordination Chemistry
Publication details, including instructions for authors and subscription information:
http://www.informaworld.com/smpp/title~content=t713455674

Synthesis, characterization, crystal structure, and biological studies of vanadium complexes with glycolic acid

Luciana R. Guilherme[a]; Antonio C. Massabni[a]; Alexandre Cuin[a]; Luiz A. A. Oliveira[a]; Eduardo E. Castellano[b]; Tassiele A. Heinrich[c]; Cláudio M. Costa-Neto[c]
[a] Instituto de Química de Araraquara, Universidade Estadual Paulista (UNESP), Araraquara-SP, Brazil [b] Instituto de Física de São Carlos, Universidade de São Paulo (USP), São Carlos-SP, Brazil [c] Faculdade de Medicina de Ribeirão Preto, Universidade de São Paulo (USP), Ribeirão Preto, Brazil

To cite this Article R. Guilherme, Luciana , Massabni, Antonio C. , Cuin, Alexandre , Oliveira, Luiz A. A. , Castellano, Eduardo E. , Heinrich, Tassiele A. and Costa-Neto, Cláudio M.(2009) 'Synthesis, characterization, crystal structure, and biological studies of vanadium complexes with glycolic acid', Journal of Coordination Chemistry, 62: 10, 1561 — 1571
To link to this Article: DOI: 10.1080/00958970802663555
URL: http://dx.doi.org/10.1080/00958970802663555

Journal of Coordination Chemistry
Vol. 62, No. 10, 20 May 2009, 1561–1571

Synthesis, characterization, crystal structure, and biological studies of vanadium complexes with glycolic acid

LUCIANA R. GUILHERME†, ANTONIO C. MASSABNI†, ALEXANDRE CUIN*†, LUIZ A.A. OLIVEIRA†, EDUARDO E. CASTELLANO‡, TASSIELE A. HEINRICH§ and CLÁUDIO M. COSTA-NETO§

†Instituto de Química de Araraquara, Universidade Estadual Paulista (UNESP), Araraquara-SP, Brazil
‡Instituto de Física de São Carlos, Universidade de São Paulo (USP), São Carlos-SP, Brazil
§Faculdade de Medicina de Ribeirão Preto, Universidade de São Paulo (USP), Ribeirão Preto, Brazil

(*Received 14 August 2008; in final form 28 October 2008*)

Synthesis, characterization, crystal structure, and biological studies of two complexes with glycolic acid are described. The solid complexes were formulated as $K_2[VO(C_2H_2O_3)(C_2H_3O_3)_2]\cdot H_2O$ (**1**) and $K_2[\{VO_2(C_2H_2O_3)\}_2]$ (**2**) and characterized by X-ray studies, Fourier transform infrared spectroscopy (FTIR), Electron paramagnetic resonance (EPR), and magnetic susceptibility. Conversion of **1** to **2** was studied in aqueous solution by UV–Vis spectroscopy and in the solid state by diffuse reflectance spectroscopy. Complex **2** contains dinuclear $[\{VO_2(C_2H_2O_3)\}_2]^{2-}$ anions in which glycolate(2−) is a five-membered chelating ring formed by carboxylate and α-hydroxy groups. The geometry around the vanadium in **2** was interpreted as intermediate between a trigonal bipyramid and a square pyramid. Vanadium(IV) is pentacoordinate in **1** as a distorted square pyramid. Complex **1** contains a vanadyl group (V=O) surrounded by two oxygens from deprotonated carboxylate and hydroxy groups forming a five-membered ring. Two oxygens from different glycolates(1−) are bonded to the (V=O) also. Biological analysis for potential cytotoxic effects of **1** was performed using Human Cervix Adenocarcinoma (HeLa) cells, a human cervix adenocarcinoma-derived cell line. After incubation for 48 h, **1** causes 90 and 95% of HeLa cells death at 20 and 200 μmol L^{-1}, respectively.

Keywords: Vanadium; Complex; Crystal structure; Glycolate; Glycolic

1. Introduction

Studies of vanadium have been motivated by its occurrence in biological systems [1]; vanadium complexes with various oxidation states are insulin-mimetic and can show anti-carcinogenic properties [2].

The coordination chemistry of vanadium in biological systems involves vanadium(IV) and vanadium(V), although there are organisms, such as tunicates,

*Corresponding author. Email: alexandre_cuin@yahoo.com

ISSN 0095-8972 print/ISSN 1029-0389 online © 2009 Taylor & Francis
DOI: 10.1080/00958970802663555

where the main oxidation state of vanadium is 3+ in blood cells [3]. Vanadium in oxidation states 4+ and 5+ interacts with metal ion binders in biological systems containing negatively charged oxygen donors similar to glycolate [4, 5], phenolate [6], phosphate [7], catecholate [8], and hydroxamate [9]. Peroxovanadium complexes with α-hydroxycarboxylic acids are of special interest as potential biochemical compounds since the anions of these acids exist in biological media and can be involved in basic biochemical processes like Krebs cycle, Cori cycle, and photorespiration [10].

Experiments carried out in the last 20 years suggest that vanadium could be considered as a representative of a new class of nonplatinum, metal antitumor agents [11].

The synthesis, structural characterization, and antitumor studies of two new oxovanadium complexes with glycolic acid are reported here.

2. Experimental

2.1. *Chemicals*

Glycolic acid (Merck), KOH (Sigma), $VOSO_4$ (Aldrich) and other reagents were used without purification.

2.2. *Synthesis*

Glycolic acid (2.0 mmol) and KOH (2.0 mmol) were dissolved in 5.0 mL of water at room temperature under stirring; $VOSO_4$ (1.0 mmol) in 5.0 mL of water was added slowly to the solution resulting in a blue solution (pH 4.2) at room temperature. This solution was concentrated at room temperature to give purple crystals of **1** suitable for X-ray studies. The purple crystals were dissolved in water at room temperature resulting in a clear blue solution from which pale green crystals of **2** were formed after about 1 week.

On the basis of the IR bands and X-ray measurements, **1** and **2** were formulated as $K_2[VO(C_2H_2O_3)(C_2H_3O_3)_2]\cdot H_2O$ and $K_2[\{VO_2(C_2H_2O_3)_2\}]$, respectively.

2.3. *Physical measurements*

IR spectra (4000–400 cm^{-1}) were recorded in a Perkin–Elmer Impact 400 Spectrophotometer using KBr pellets. Electron paramagnetic resonance (EPR) spectra were recorded in a Bruker ESP 300E X-band Spectrometer in the solid state at 77 K and in solution at 298 K. Magnetic susceptibilities were recorded in a Johnson–Matthey MK II balance using the modified Gouy's method [12]. UV–Vis spectra were obtained at room temperature in a Hewlett-Packard HP 8453A spectrophotometer operating from 1200 to 200 nm using quartz cells and a Perkin-Elmer Lambda 14P equipment for the solid samples.

2.4. *Preparation of the solutions*

Fresh stock solutions of vanadium sulfate and **1** and **2** were prepared by dissolution of each solid in suitable volumes of phosphate-buffered saline solution (PBS), immediately

before each experiment. Solutions of final different concentrations of the complexes were obtained by dilution of each stock solution directly into the cell medium. PBS was used as the vehicle for all biological assays.

2.5. *Cell culture*

The Human Cervix Adenocarcinoma (HeLa) cells were cultured as described [13] with few modifications. Briefly, cells were cultured at 37°C in a humidified atmosphere containing 5% CO_2 and grown in 75 cm^2 flasks with Dulbecco's modified Eagle's medium (DMEM) at pH 7.2, supplemented with 10% of fetal calf serum (FCS) containing gentamicin (10 $\mu g\,mL^{-1}$) as an antibiotic.

2.6. *Cytotoxic assays*

Cells were detached and seeded in a 48-well plate (2.0×10^4 cells/well) and after 24 h the medium was exchanged. Compounds in different concentrations or the vehicle were incubated for a period of 48 h. After this period 50.0 μL of 1-(4,5-dimethylthiazol-2-yl)-3,5-diphenylformazan (MTT) solution (5.0 $mg\,mL^{-1}$ in PBS) were added to each well, which was incubated for an additional 3 h [14]. Subsequently, the medium was removed, cells were washed two times with PBS, and 200 μL of isopropanol-HCl (0.040 $mol\,L^{-1}$) were added. Cell viability was determined by absorbance measurements at 570 nm and correlated to the ability of reducing MTT to produce a colored compound.

2.7. *Crystal structure analysis*

Both crystals were mounted on an Enraf–Nonius Kappa–CCD Diffractometer provided with graphite monochromated Mo-Kα ($\lambda = 0.71073$ Å) radiation. Final unit cell parameters were based on all reflections. Data collections were made using the *COLLECT* program [15]; integration and scaling of the reflections were performed with the HKL Denzo-Scalepack system of programs [16]. Absorption corrections were carried out using the Gaussian method [17]. Both structures were solved by direct methods with *SHELXS-97* [18] and refined by full-matrix least squares on F^2 by *SHELXL-97* [19]. Nonwater hydrogen atoms were stereochemically positioned and the ones from water in **1** form a difference map. All data were refined using the riding model. Data collection and experimental details are summarized in table 1. Projections of **1** and **2** are shown in figures 1 and 2 (prepared using ORTEP-3 for windows [20]), and selected interatomic distances and angles for **1** and **2** are shown in tables 2 and 3, respectively. Complex **2** is sited on a crystallographic center of symmetry.

3. Results and discussion

Complex **1** contains vanadium(IV), whereas **2** contains vanadium(V). The vanadium oxidation state changes from (IV) to (V) when **1** is transformed into **2** in aqueous solution.

Table 1. Crystal data and structure refinements for **1** and **2**.

	1	**2**
Empirical formula	$C_6H_{10}K_2O_{11}V$	$C_2H_2KO_5V$
Formula weight	387.28	196.07
Temperature (K)	296(2)	293(2)
Wavelength (Å)	0.71073	0.71073
Crystal system, space group	Monoclinic, P_21/a	Monoclinic, P_21/a
Unit cell dimensions (Å, °)		
a	9.8646(6)	5.9347(3)
b	14.3610(10)	11.5853(4)
c	10.0970(10)	8.3215(3)
β	115.477(4)	100.420(3)
V (Å^3)	1291.3(2)	562.71(4)
Z, Calculated density (Mg m^{-3})	4, 1.992	4, 2.314
Absorption coefficient (mm^{-1})	1.466	2.443
F(000)	780	384
Crystal size (mm^3)	$0.14 \times 0.09 \times 0.03$	$0.262 \times 0.170 \times 0.100$
θ range for data collection	3.61–26.00 °	3.05–26.00 °
Limiting indices	$-12 \le h \le 12$, $-16 \le k \le 17$, $-10 \le l \le 12$	$-7 \le h \le 7$, $-14 \le k \le 12$, $-9 \le l \le 10$
Reflections collected/unique	6889/2530 [$R_{(int)} = 0.0518$]	3661/1081 [$R_{(int)} = 0.0321$]
Completeness to $\theta = 26.00$	99.6%	97.3%
Max and min transmission	0.9519 and 0.8211	0.751 and 0.647
Refinement method	Full-matrix least-squares on F^2	Full-matrix least-squares on F^2
Data/restraints/parameters	2530/0/181	1081/0/82
Goodness-of-fit on F^2	1.027	1.085
Final R indices [$I > 2\sigma(I)$]	$R_1 = 0.0441$, $wR_2 = 0.1028$	$R_1 = 0.0238$, $wR_2 = 0.0637$
R indices (all data)	$R_1 = 0.0726$, $wR_2 = 0.1181$	$R_1 = 0.0248$, $wR_2 = 0.0644$
Largest diff. peak and hole (e Å^{-3})	0.454 and −0.596	0.246 and −0.374

Notes: R_1 values are based on F values while wR_2 values are based on F^2.
$a = 0.062$ and $b = 0.000$ for **1**, $a = 0.313$ and $b = 0.413$ for **2**.
$R_1 = \Sigma w||F_0| - |F_c||/\Sigma|F_0|$,
$wR_2 = \{\Sigma w(F_o^2 - F_c^2)^2/\Sigma w(F_o^2)^2\}^{1/2}$
$w = 1/\sigma^2(F_o)^2 + (aP)^2 + bP$
$P = [2F_c^2 + \max(F_o^2, 0)]/3$.

3.1. *IR spectra*

The main bands of the IR spectra of the two complexes are listed in table 4. Bands corresponding to the asymmetric and symmetric stretching modes of a monodentate carboxylate (COO^-) were observed for both complexes; the Δ value [$\Delta = \nu_{as}(COO^-) - \nu_s(COO^-)$] is larger than 200 cm^{-1} [21]. The bands at 1072 and 1084 cm^{-1} for **1** and **2**, respectively, are assigned to coordination of (C–O$^-$) of the deprotonated α-hydroxy group. The bands at 945 and 939 cm^{-1} were assigned to the stretching frequencies of the terminal V–O bonds for **1** and **2**, respectively. The band at 760 cm^{-1} was assigned to the (V–O–V) stretching frequency for **2** [22].

3.2. *EPR spectra and magnetic susceptibility*

Electron paramagnetic resonance spectrum of **1** in aqueous solution shows a typical signal of d^1 vanadium(IV) with eight lines (nuclear spin $I = 7/2$) with $g = 1.998$ and $A = 102$G (figure 3). Such results are evidence of the presence of a monomeric oxovanadium(IV) group. The magnetic moment expected for a vanadyl(IV) complex

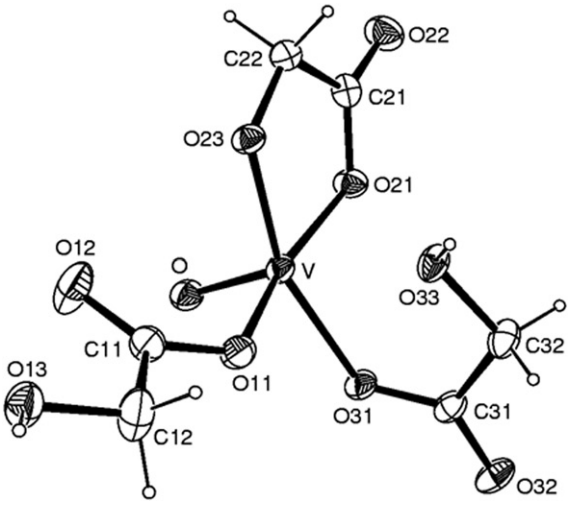

Figure 1. ORTEP projection for **1** showing the labeling scheme. Displacement ellipsoids are drawn at 30% probability. For clarity, the potassium ions and the water molecule were not included.

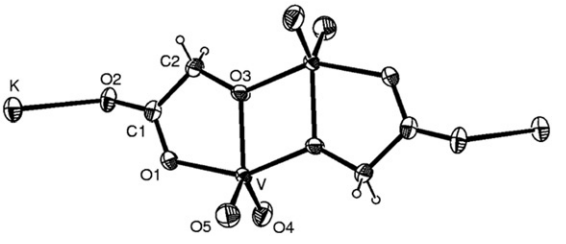

Figure 2. Molecular structure for **2**. The atoms of the asymmetric unit on the left are labeled.

Table 2. Bond lengths and angles for **1**.

V–O	1.611(3)
V–$O_{(23)}$	1.919(3)
V–$O_{(21)}$	2.002(2)
V–$O_{(11)}$	2.044(2)
V–$O_{(31)}$	2.046(3)
V–$O_{(33)}$	2.243(2)
O–V–$O_{(23)}$	105.56(12)
O–V–$O_{(21)}$	99.02(13)
$O_{(23)}$–V–$O_{(21)}$	81.81(10)
O–V–$O_{(11)}$	98.25(12)
$O_{(23)}$–V–$O_{(11)}$	92.59(10)
$O_{(21)}$–V–$O_{(11)}$	162.71(11)
O–V–$O_{(31)}$	93.61(12)
$O_{(23)}$–V–$O_{(31)}$	159.73(11)
$O_{(21)}$–V–$O_{(31)}$	88.83(10)
$O_{(11)}$–V–$O_{(31)}$	91.10(10)
O–V–$O_{(33)}$	166.97(12)
$O_{(23)}$–V–$O_{(33)}$	87.44(10)
$O_{(21)}$–V–$O_{(33)}$	81.62(10)
$O_{(11)}$–V–$O_{(33)}$	81.79(10)
$O_{(31)}$–V–$O_{(33)}$	73.37(10)

Table 3. Bond lengths and angles for **2**.

$V–O_{(5)}$	1.620(3)	$O_{(5)}–V–O_{(1)}$	99.24(15)
$V–O_{(4)}$	1.626(3)	$O_{(4)}–V–O_{(1)}$	97.57(14)
$V–O_{(3)}{}^{\#1}$	1.950(3)	$O_{(3)}{}^{\#1}–V–O_{(1)}$	147.24(12)
$V–O_{(1)}$	1.973(3)	$O_{(5)}–V–O_{(3)}$	125.25(17)
$V–O_{(3)}$	2.008(3)	$O_{(4)}–V–O_{(3)}$	126.08(17)
$O_{(5)}–V–O_{(4)}$	108.65(18)	$O_{(3)}{}^{\#1}–V–O_{(3)}$	70.50(13)
$O_{(5)}–V–O_{(3)}{}^{\#1}$	99.46(16)	$O_{(1)}–V–O_{(3)}$	76.74(12)
$O_{(4)}–V–O_{(3)}{}^{\#1}$	101.58(16)	$V^{\#1}–O_{(3)}–V$	109.50(13)

Note: Symmetry code: #1 $-x+1, -y, -z$.

Table 4. Infrared bands for **1** and **2**.

Complex	$\nu(H_2O)$	$\nu_{as}(COO^-)$	$\nu_s(COO^-)$	$\Delta\nu(cm^{-1})$	$\nu(C–O^-)$	$\nu(V{=}O)$	$\nu(V–O–V)$
1	3350 (s)	1632 (vs)	1364 (s)	268	1072 (s)	945 (s)	–
2	3437 (s)	1680 (vs)	1348 (vs)	332	1084 (s)	939 (s)	760 (m)

Note: $\Delta\nu = \nu_{as}(COO^-) - \nu_s(COO^-)$.

is 1.73 BM [23] and the value found for **1** is 1.54 BM. Complex **2** is EPR-inactive and diamagnetic because it contains vanadium(V) (a d^0 system).

When **1** was dissolved in water the intensity of the lines of the EPR spectrum gradually reduces, indicating that **1** was oxidized by atmospheric O_2 and the binuclear **2** was formed.

3.3. *UV–Vis spectra*

The UV–Vis spectrum of **1** in the solid state (supplementary material) exhibits four bands typically found for vanadium(IV) complexes (a d^1 system). The weak absorption band at 854 nm is assigned to a d–d transition ($d_{xy} \rightarrow d_{yz}$) and the weak absorption bands at 556 and 345 nm are assigned to the d–d transitions ($d_{xy} \rightarrow d_{x2-y2}$) and ($d_{xy} \rightarrow d_{z2}$), respectively [24]. The band at 258 nm is assigned to a LMCT process. The UV–Vis spectrum of **2** in the solid state exhibits only a strong absorption band at 270 nm assigned to a LMCT process.

Conversion of **1** to **2** was observed spectrophotometrically in the solid state and followed in aqueous solution (supplementary material). Characteristic bands at 854 and 556 nm observed after dissolution of **1** in water shift to 788 and 565 nm, respectively. The intensity of the bands decrease with time. After approximately 2 h, the intensity of the absorption at 788 nm almost stabilized but decreased slowly until it practically disappears after more than 4 days. This kinetic behavior suggests the formation of a relative stable intermediate followed by its slow conversion to binuclear **2**, in two consecutive steps, as shown in scheme 1.

The initial spectral changes that followed dissolution of **1** in water were interpreted as being due to loss of the monodentate glycolate coordinated to vanadium, which was substituted by water, giving rise to an intermediate. The spectral changes that occur in longer periods of time were interpreted as being due to slow oxidation

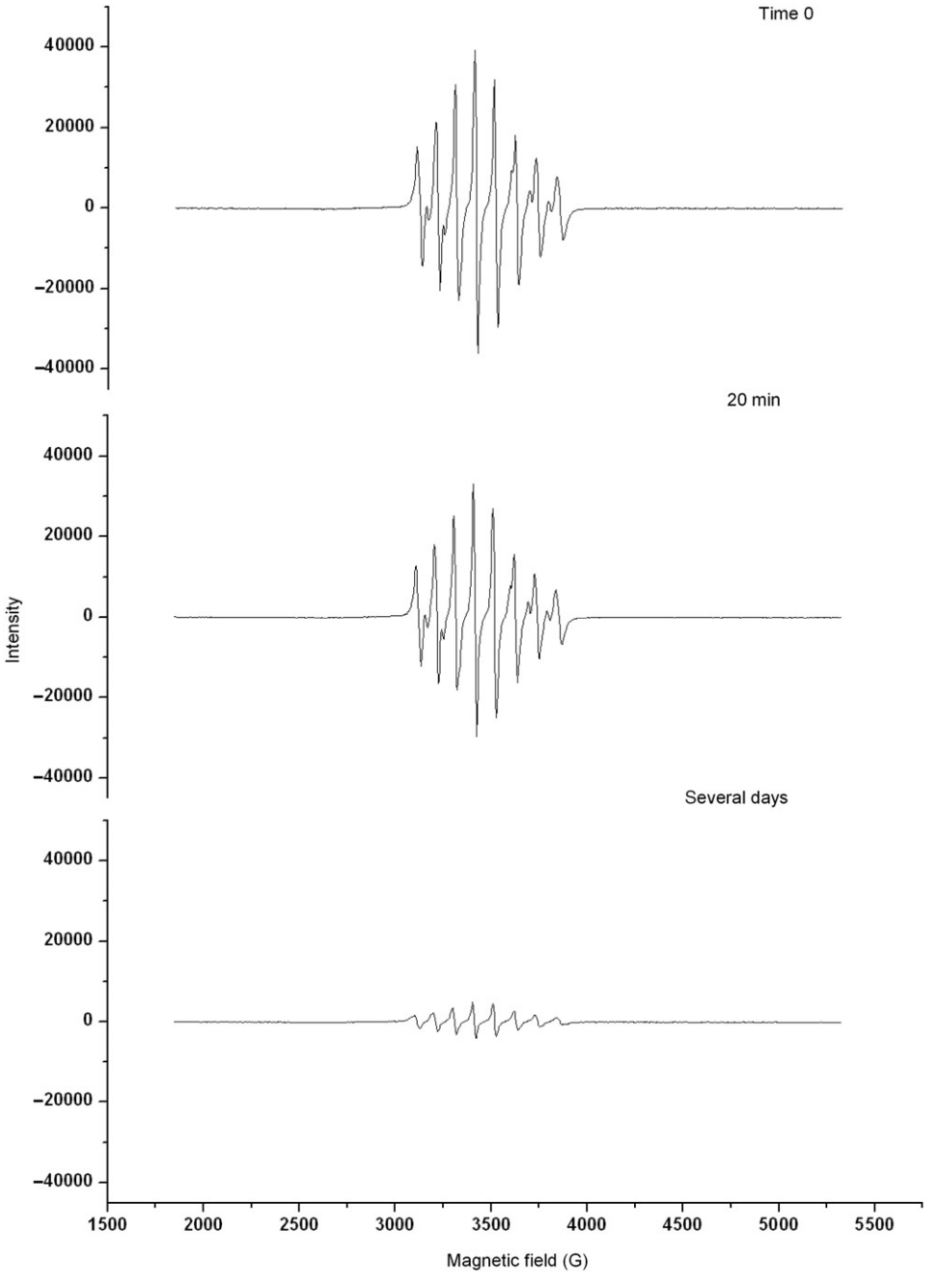

Figure 3. X-band EPR spectrum for **1** in aqueous solution at 298 K.

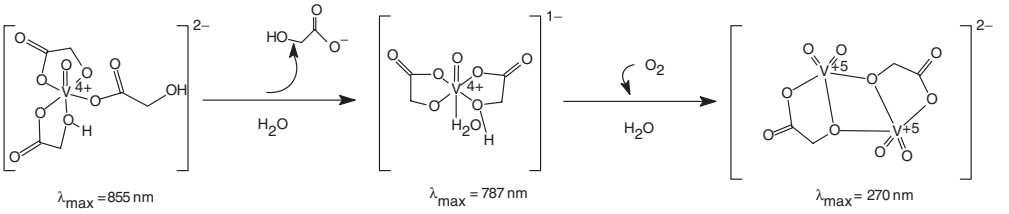

Scheme 1. Consecutive steps for the conversion of **1** in **2**.

of vanadium(IV) to vanadium(V) by atmospheric oxygen, giving the binuclear species **2** as the final product.

3.4. *X-ray structures*

The molecular structure of **1** is a monomeric arrangement of three glycolates and one oxovanadium(IV) [V–O(oxo), 1.611(3) Å] (figure 1). The distorted square-pyramidal geometry around vanadium can be visualized as an equatorial plane, formed exclusively by oxygen atoms of the glycolate anions, and an axial direction, occupied by the oxo. Two coordination points of the equatorial plane are occupied by the completely deprotonated glycolate anion, coordinated to the central metal through monodentate carboxylate and α-hydroxy groups forming a five-membered ring as in the case of a glycolate molybdenum complex [21]. The third and fourth coordination positions of the equatorial plane around the metal are occupied by the monodentate carboxylate groups of the monodeprotonated glycolate anion. The metal–oxygen distances are in the range 1.913–2.046 Å. The geometric parameter τ is equal to 0.05, calculated using the formula $\tau = (\beta - \alpha)/60$, where β and α are the O_{11}–V–O_{21} and O_{23}–V–O_{31} angles, respectively (table 2) [25]. Two potassium ions complete the charge balance of $[VO(C_2H_2O_3)(C_2H_3O_3)_2]^{2-}$. There is also a hydration water molecule completing the structure. For a V^{IV}–citrate complex [26] the geometry was considered as distorted octahedral. The longest distance for the V–O bond is 2.303 Å and the angle for the axial axis is 172.3°. Distorted octahedral geometry could also be considered for **1** if the sixth coordination position of the V–O_{33} would be considered. The V–O_{33} distance and the O–V–O_{33} angle are 2.243 Å and 166.97°, respectively. Both the V–O_{33} bond and the O–V–O_{33} angle compare very well with the values described by Burojevic *et al.* [26].

A perspective view (ORTEP) of **2** is given in figure 2. In this case, τ is equal to 0.35 with β and α values corresponding to O_1–V–$O_3^{\#1}$ and O_4–V–O_3 angles, respectively (table 3) [25]. The τ value indicates that **2** is an intermediate between a trigonal bipyramidal and a square pyramidal [27, 28]. The structure of **2** contains centrosymmetric dinuclear $[\{VO_2(C_2H_2O_3)\}_2]^{2-}$ anions such as for a rubidium dioxovanadium(V) glycolate complex, described by Biagioli *et al.* [29]. Biagioli's complex belongs to the triclinic system and **2** is monoclinic. Table 3 lists pertinent bond length and bond angle data, whereas the basic structural features of **2** and the Biagioli complex are summarized in table 5.

The V=O (oxo) bond distances observed for **2** [1.620 and 1.626 Å for V_1–O_5 and V_1–O_4] are in the range usually found for similar binuclear complexes reported in the

Table 5. Comparison of structural parameters of **2** and a similar complex.

	$Rb_2[(VO_2)_2(C_2H_2O_3)_2]$	**2**
$V–O_{(4)}$	1.614(2)	1.626(3)
$V–O_{(5)}$	1.614(2)	1.620(3)
$V–O_{(1)}$	1.979(2)	1.973(3)
$V–O_{(3)}$	1.998(2)	2.008(3)
$V–O_{(3)}{}^{\#1}$	1.944(2)	1.950(3)
$O_{(5)}–V–O_{(4)}$	107.87(11)	108.65(18)
$O_{(5)}–V–O_{(3)}{}^{\#1}$	99.79(9)	99.46(16)
$O_{(4)}–V–O_{(3)}{}^{\#1}$	100.40(10)	101.58(16)
$O_{(5)}–V–O_{(3)}$	128.6(10)	125.25(17)
$O_{(4)}–V–O_{(3)}$	123.5(10)	126.08(17)
$O_{(3)}{}^{\#1}–V–O_{(3)}$	71.14(7)	70.50(13)
$O_{(1)}–V–O_{(3)}$	76.71(7)	76.74(12)
$V–O_{(3)}–V^{\#1}$	108.86(7)	109.50(13)

Note: Symmetry code: #1 $-x+1, -y, -z$.

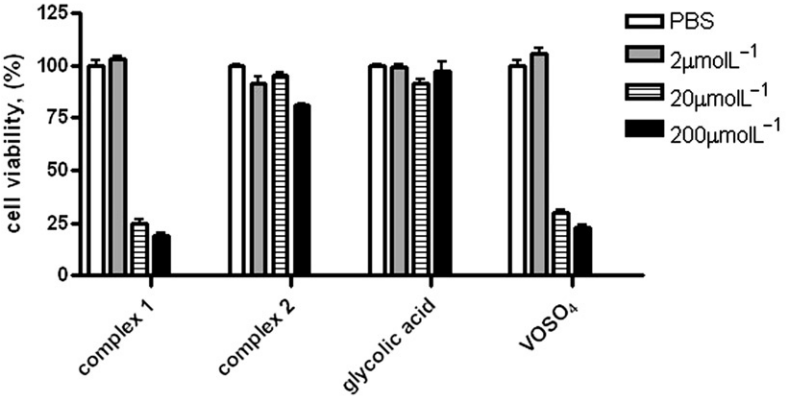

Figure 4. Cytotoxic analysis for **1** and **2**. The data represent the averages of four independent experiments performed in duplicate.

literature [29, 30] [1.614 and 1.614 Å for the glycolato(2−) complex; 1.610 and 1.619 Å for the malato(2−) complex; 1.617 and 1.635 Å for the lactato(2−) complex; 1.611 and 1.623 Å for the citrate complex, respectively]. A comparison of these bond distances with the longer ones observed for the $V_1–O_1$ and $V_1–O_3$ bonds [1.973 and 1.950 Å, respectively] shows the existence of stronger interactions, reinforcing that $V_1–O_5$ and $V_1–O_4$ are double bonds.

3.5. *Biological assays*

Cytotoxic assays were performed for **1** at several concentrations against HeLa cells *in vitro* (figure 4). The data show that after incubation for 48 h, **1** causes 90 and 95% of cell death at 20 and 200 μmol L^{-1}, respectively. Similar behavior was observed for vanadyl sulfate. Complex **2** and free glycolic acid showed no significant cytotoxic activity even at 200 μmol L^{-1}.

4. Conclusions

Glycolic acid reacts with oxovanadium(IV) to form the purple complex **1** that absorbs at 855 nm. This peak disappears after several days in the presence of atmospheric oxygen. Formation of a new species was followed by increasing absorption at 270 nm. The new species was identified as the binuclear vanadium(V) complex **2**. EPR spectroscopic studies provided evidence that the conversion involves the change of a paramagnetic vanadium species **1** to a diamagnetic d^0 vanadium (**2**). The crystal structures of both complexes were determined, confirming the monomeric and dimeric nature of **1** and **2**, respectively. Considering the cytotoxic assays *in vitro* a concentration of 20 μmol L^{-1} of **1** caused 90% of HeLa cells death after incubation for 48 h.

Supplementary materials

Supplementary crystallographic data are available through the Cambridge Crystallographic Data Centre, CCDC 698560 for **1** and CCDC 698561 for **2**. Copies of this information may be obtained free of charge from the Director, CCDC 12 Union Road, Cambridge, CB2 1EZ, UK (Fax +44 12-2333-6033; E-mail: deposit@ccdc.cam.ac.uk or http://www.ccdc.cam.ac.uk).

Acknowledgements

The authors are grateful to "Coordenação de Aperfeiçoamento de Pessoal de Nível Superior – CAPES" for financial support.

References

[1] T.S. Smith, R. LoBrutto, V.L. Pecoraro. *Coord. Chem. Rev.*, **228**, 1 (2002).
[2] C. Orvig, K.H. Thompson, M. Battell, J.H. Mcneill. *Met. Ions Biol. Syst.*, **31**, 575 (1995).
[3] N.D. Chasteen. *Met. Ions Biol. Syst.*, **31**, 231 (1995).
[4] T. Kiss, P. Buglyó, D. Sanna, G. Micera, P. Decock, D. Dewaele. *Inorg. Chim. Acta*, **239**, 145 (1995).
[5] A. Cuin, A.C. Massabni, C.Q.F. Leite, D.N. Sato, A. Neves, B. Szpoganicz, M.S. Silva, A.J. Bortoluzzi. *J. Inorg. Biochem.*, **101**, 291 (2007).
[6] S. Cakir, E. Bicer, P. Naumov, O. Cakir. *J. Coord. Chem.*, **55**, 1461 (2002).
[7] L. Mafra, F.A.A. Paz, F.N. Shi, C. Fernandez, T. Trindade, J. Klinowski, J. Rocha. *Inorg. Chem. Commun.*, **9**, 34 (2006).
[8] G. Asgedom, A. Sreedhara, C.P. Rao, E. Kolehmainen. *Polyhedron*, **15**, 3731 (1996).
[9] P. Buglyo, N. Potari. *Polyhedron*, **24**, 837 (2005).
[10] P. Schwendt, P. Svancarek, I. Smatanova, J. Marek. *J. Inorg. Biochem.*, **80**, 59 (2000).
[11] A.M. Evangelou. *Crit. Rev. Oncol. Hemat.*, **42**, 249 (2002).
[12] J. Woolcock, A. Zafar. *J. Chem. Educ.*, **69**, A176 (1982).
[13] P.P. Corbi, A.C. Massabni, A.G. Moreira, F.J. Medrano, M.G. Jasiulionis, C.M. Costa-Neto. *Can. J. Chem.*, **83**, 104 (2005).
[14] T. Mosmann. *J. Immun. Met.*, **65**, 55 (1983).
[15] Enraf-Nonius. *COLLECT. Nonius BV*, Delft, The Netherlands (1997–2000).
[16] Z. Otwinowski, W. Minor. In *Methods in Enzymology*, C.W. Carter Jr., R.M. Sweet (Eds), Vol. 276, pp. 307–326, Academic Press, New York (1997).

[17] P. Coppens, L. Leiserowitz, D. Rabinovich. *Acta Cryst*., **18**, 1035 (1965).
[18] G.M. Sheldrick. *SHELXS-97. Program for Crystal Structure Resolution*, Univeristy of Göttingen, Germany (1997).
[19] G.M. Sheldrick. *SHELXL-97. Program for Crystal Structures Analysis*, University of Göttingen, Germany (1997).
[20] L.J. Farrugia. ORTEP-3 for Windows, *J. Appl. Cryst*., **30**, 565 (1997).
[21] A. Cuin, A.C. Massabni. *J. Coord. Chem*., **60**, 1933 (2007).
[22] J.M. Arrieta. *Polyhedron*, **11**, 3045 (1992).
[23] J. Selbin. *Chem. Rev*., **65**, 153 (1965).
[24] C.J. Ballhausen, H.B. Gray. *Inorg. Chem*., **1**, 111 (1962).
[25] A.W. Addison, T.N. Rao, J. Reedijk, J. van Rijn, G.C. Verschoor. *J. Chem. Soc., Dalton Trans*., 1349 (1984).
[26] S. Burojevic, I. Shwek, A. Bino, D.A. Summers, R.C. Thompson. *Inorg. Chim. Acta*, **251**, 75 (1996).
[27] M. Kaliva, C. Gabriel, C.P. Raptopoulou, A. Terzis, A. Salifoglou. *Inorg. Chim. Acta*, **361**, 2631 (2008).
[28] M. Kaliva, E. Kyriakakis, C. Gabriel, C.P. Raptopoulou, A. Terzis, J.P. Tuchagues, A. Salifoglou. *Inorg. Chim. Acta*, **359**, 4535 (2006).
[29] M. Biagioli, L. Strinna-Erre, G. Micera, A. Panzanelli, M. Zema. *Inorg. Chim. Acta*, **310**, 1 (2000).
[30] D.W. Wright, R.T. Chang, S.K. Mandal, W.H. Armstrong, W.H. Orme-Johnson. *J. Biol. Inorg. Chem*., **1**, 143 (1996).